EPJ manuscript No.
(will be inserted by the editor)

Measurement of J/ψ Production in Proton-Proton Collisions by the PHENIX Experiment

Nichelle Bruner for the PHENIX Collaboration

University of New Mexico, Albuquerque, NM 87131, USA

Received: date / Revised version: date

Abstract. The PHENIX experiment at the Relativistic Heavy Ion Collider has measured J/ψ production in proton-proton collisions at $\sqrt{s} = 200$ GeV using data from the 2001–2002 collider run. Distributions of rapidity and transverse momentum are presented and compared with theoretical predictions. The total cross section and mean p_T are calculated and compared to fixed-target results. The total J/ψ cross section is 4.0 $\pm$ 0.6(stat) $\pm$ 0.6(sys) $\pm$ 0.4(abs) μb. The mean p_T is 1.80 $\pm$ 0.23(stat) $\pm$ 0.16(sys) GeV/c.

PACS. 25.75.Dw Particle and resonance production

1 Introduction

Theoretical interest in the J/ψ production mechanism was raised when the CDF measurements of prompt J/ψ and $\psi(2S)$ differential cross sections [1] were much larger than the Color Singlet Model (CSM) prediction [2]. The Color Octet Model (COM) and Color Evaporation Model have had more success matching the high p_T data [3,4]. However, understanding the production mechanisms will require total cross section and $\langle p_T \rangle$ measurements. These existed only for fixed target energies, $\sqrt{s}$= 7-38.8 GeV.

The PHENIX detector can provide data at Relativistic Heavy Ion Collider (RHIC) energies with broad coverage in rapidity and p_T. This should enable testing of various J/ψ production models as well as provide a baseline for the PHENIX spin and heavy ion physics programs.

In this paper, we present the first measurement of $pp \to J/\psi + X$ at $\sqrt{s} = 200$ GeV from RHIC. The data were recorded in the 2001-2002 RHIC proton-proton run using the two PHENIX central arm spectrometers and one forward muon spectrometer. These measurement results were submitted to Phys. Rev. Lett. [5].

2 The PHENIX Detector

The $pp \to J/\psi + X$ measurement was performed in two channels at PHENIX, $J/\psi \to e^+e^-$ and $J/\psi \to \mu^+\mu^-$. We describe the relevant detector components and triggering for each channel. Details of the entire PHENIX detector can be found in Ref. [6].

The central arm spectrometers were used to measure $J/\psi \to e^+e^-$. The central arms measure electrons, charged hadrons, and photons in $|\eta| < 0.35$ in pseudo-rapidity and in $\pi/2$ in azimuth for each arm. Electrons are identified by matching charged particle tracks from tracking sub-systems to energy deposits in the Electromagnetic Calorimeter (EMC) and to rings in the Ring Imaging Cerenkov Detector (RICH). Electrons in our data sample come from a coincidence of the minimum bias interaction trigger and an electron level 1 trigger. The minimum bias trigger required one hit in the Beam-Beam counters (BBC) on each side of the interaction vertex. The electron level 1 trigger required there be energy greater than 0.75 GeV in a 2×2 tile of EMC towers or greater than 2.1 GeV in a 4×4 tile. After quality assurance cuts and a vertex requirement of $|z_{vertex}| < 35$, 82 nb^{-1} of data remained for the $J/\psi \to e^+e^-$ analysis.

A forward muon arm was used to measure $J/\psi \to \mu^+\mu^-$. This arm spans $-2.2 < \eta < -1.2$ in pseudo-rapidity with full azimuthal coverage. A muon arm is comprised of a precision tracking detector followed by a muon identifier. This muon identifier is composed of five layers of transversely-oriented proportional tubes separated by steel absorbers to provide hadron rejection. Track stubs in the identifier are used to seed tracks in the tracking detector. Muons in our data sample come from a coincidence in the BBC and a muon level 1 trigger. The muon trigger required at least two deeply penetrating roads in separate azimuthal quadrants of the muon identifier. After quality assurance cuts and a vertex requirement of $|z_{vertex}| < 38$, 67 nb^{-1} of data remained for the $J/\psi \to \mu^+\mu^-$ analysis, discussed with e^+e^- in the next section.

3 Analysis Procedure

The J/ψ differential cross section as a function of p_T and rapidity, y, is given by

$$B_{ll}\frac{d^2\sigma_{J/\psi}}{dydp_T} = \frac{N_{J/\psi}}{(\int \mathcal{L}dt)\Delta y \Delta p_T}\frac{1}{\epsilon_{bias}\epsilon_{lvl1}}\frac{1}{A\epsilon_{reco}}, \quad (1)$$

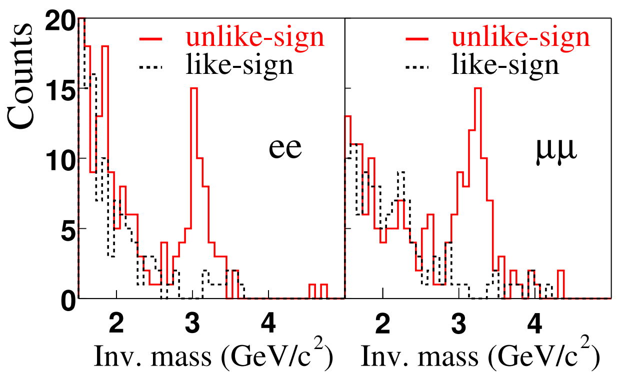

Fig. 1. The invariant mass spectra for ee (left) and $\mu\mu$ (right). The solid histograms represent unlike-sign pairs. The dashed histograms represent like-sign combinations.

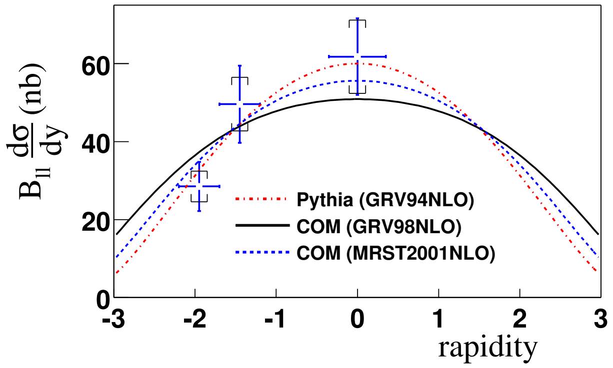

Fig. 2. J/ψ differential cross section as a function of rapidity. The value for $y = 0$ is from e^+e^-. The two values for $y < 0$ are from $\mu^+\mu^-$. Brackets represent the systematic uncertainty. The solid and dashed curves are predictions from the Color Octet Model for two parton distribution functions. The dot-dash line is the Pythia prediction. All curves are normalized to the PHENIX data.

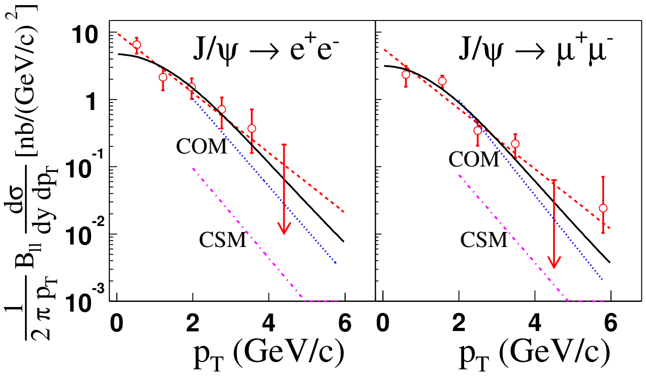

Fig. 3. The p_T distribution of the J/ψ as measured in the electron (left) and muon (right) decay channels. The solid line is a fit to $1/(2\pi p_T)d\sigma/dp_T = A(1 + (p_T/B)^2)^{-6}$, a phenomenological description of the fixed-target data. Predictions from the CSM (dot-dashed) and COM (dotted) are also shown [10].

where B_{ll} is the J/ψ leptonic branching ratio, $\int \mathcal{L}dt$ is the integrated luminosity measured by the minimum bias trigger, Δy and Δp_T are the rapidity and p_T bins, $N_{J/\psi}$ is the number of measured J/ψ in a given bin, ϵ_{bias} is the minimum bias trigger efficiency for an event containing a J/ψ, ϵ_{lvl1} is the level-1 trigger efficiency for detecting a J/ψ, and $A\epsilon_{reco}$ is the J/ψ acceptance × reconstruction efficiency. The values for these variables, given below, include systematic uncertainties.

Although the value of $\int \mathcal{L}dt$ is different for the electron and muon analyses, the uncertainty on both values is ±9.6% Also common to both analyses is ϵ_{bias}, which we estimated in two ways, see Ref. [5]. From these, we use $\epsilon_{bias} = 0.75 \pm 3\%$, whichis independent of p_T.

For the muon analysis, the combined value of $A\epsilon_{reco} \times \epsilon_{lvl1}$ was determined from Pythia [7] and GEANT simulations for each bin in p_T and y. The range of values is 0.038 - 0.017 ± 13%.

For the electron analysis, ϵ_{lvl1} as a function of p_T is in the range 0.87-0.90 ± 5% for 2×2 EMC tiles and 0.30-0.74 ± 36% for 4×4 tiles. From GEANT simulation, $A\epsilon_{reco}$ is 0.026-0.010 ± 13%.

$N_{J/\psi}$ is determined as the number of unlike-sign lepton pairs minus the number of like-sign pairs in each bin. Fig. 1 shows the invariant mass as a function of p_T for ee and $\mu\mu$ like- and unlike-sign pairs.

4 Results

We divide data from the muon analysis into two rapidity bins and use the electron data as a third bin. The resulting J/ψ differential cross section is shown in Fig. 2. The COM curves, using two representative parton distribution functions (PDFs), are theoretical shape predictions normalized to our data for comparison. Since gluon fusion is the dominant process in all models, the rapidity shape depends mostly on the PDF and not the model. Fig. 2 shows that we will need more statistics to be sensitive to the differences in PDFs. A distribution calculated using Pythia was also normalized to our data in Fig. 2. The total J/ψ cross section is determined from this to be 4.0 ± 0.6(stat) ± 0.6(sys) ± 0.4(abs) μb.

The J/ψ p_T distributions are shown in Fig. 3 separately for the electron and muon analyses. Both are compared to CSM and COM predictions, which are limited to $p_T > 2$ GeV/c [10]. The COM is consistent with data. The solid line in Fig. 3 is a phenomenological fit of a form used at fixed target energies [8]. The combined value from fits to the electron and muon data is $\langle p_T \rangle = 1.80 \pm 0.23$(stat) ± 0.16(sys) GeV/c.

The total cross section and $\langle p_T \rangle$ measured by PHENIX are compared to previous experiments [9] in Fig. 4. While there are no theoretical predictions for $\langle p_T \rangle$, we can compare the total cross sections to the COM with various choices of QCD parameters. To get good agreement with data, we set the renormalization scale equal to the charm quark mass and use factorization scale $Q = 3.1$ GeV with

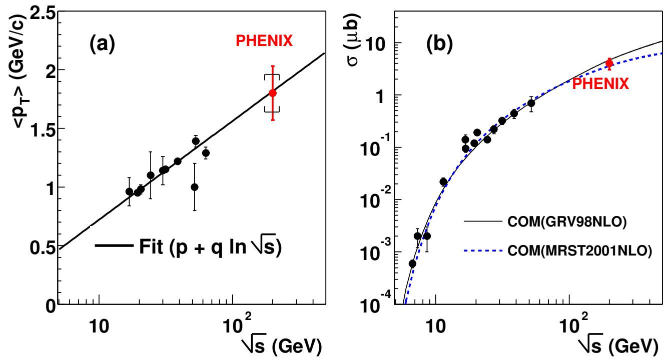

Fig. 4. J/ψ mean p_T (a) and cross section (b) as a function of $\sqrt{s}$. In the linear fit of mean p_T, p=0.53 and q=0.19.

PDF GRV98NLO, and $Q = 2.3$ GeV with MRST2001NLO.

5 Conclusion and Outlook

We presented the first $pp \to J/\psi + X$ result from RHIC. In Run 2 data, we measured the total J/ψ cross section to be 4.0 ± 0.6(stat) ± 0.6(sys) ± 0.4(abs) μb. We measured a mean p_T of 1.80 ± 0.23(stat) ± 0.16(sys) GeV/c. We compared the J/ψ y and p_T spectra to previous experiments and theoretical predictions. The y distribution is consistent with competing PDFs. The p_T distribution and total cross section are consistent with the COM.

This measurement is the first in a program which will include different collision energies and species. In the near term, results can be anticipated from RHIC Run 3, which completed in May 2003. In this run, PHENIX collected 2.7 nb^{-1} of deuterium-gold ion collisions at $\sqrt{s} = 200$ GeV and 0.35 pb^{-1} of p-p collisions also at $\sqrt{s} = 200$ GeV. In addition to the increased integrated luminosity, PHENIX installed its second muon arm for Run 3. This additional muon arm covers $1.2 < y < 2.4$, more than doubling the muon acceptance. Thus the statistics, p_T reach, and y coverage will be increased.

References

1. CDF Collaboration, F. Abe *et al.*, Phys. Rev. Lett. **79** (1997) 572.
2. E. Braaten *et al.*, Ann. Rev. Nucl. Part. Sci. **46** (1996) 197.
3. G. T. Bodwin *et al.*, Phys. Rev. **D51** (1995) 1125; erratum Phys. Rev. **D55** (1997) 5853.
4. J. F. Amundson *et al.*, Phys. Lett. **B390** (1997) 323.
5. K. Adler *et al.*, submitted to Phys. Rev. Lett. (2003); hep-ex/0307019.
6. K. Adcox *et al.*, Nucl. Inst. Meth. **A499** (2003) 469.
7. T. Sjostrand, Comp. Phys. Comm. **135** (2001) 238.
8. A. Gribushin *et al.*, Phys. Rev. **D62** (2000) 012001 and references therein.
9. R. Vogt, Phys. Repts. **310** (1999) 197; G.A. Schuler, hep-ph/9403387, and references therein.
10. G. Nayak *et al.*, Phys. Rev. **D68** (2003) 034003.